Model Systems with Extreme Aspect Ratio, Tunable Geometry, and Surface Functionality for a Quantitative Investigation of the Lotus Effect

Achim Walter Hassel,*,† Srdjan Milenkovic,† Ulrich Schürmann,‡ Henry Greve,‡ Vladimir Zaporojtchenko,‡ Rainer Adelung,‡ and Franz Faupel‡

Max-Planck-Institut für Eisenforschung GmbH, Düsseldorf, Germany and Christian-Albrechts-Universität, Kiel, Germany

Received June 6, 2006. In Final Form: August 4, 2006

Superhydrophobicity and superhydrophilicity of surfaces are key properties for fabrication of self-cleaning surfaces (Lotus effect). It is well known that the mechanism behind this is based on the surface roughness and surface functionalization. To obtain an understanding of the details of the underlying mechanism, a metal system based on a eutectic is suggested. In this study, a wide range tunability of its needlelike narrow size distributed nanostructure is demonstrated. The length of the needles as well as their density can be varied independently. In addition, an important parameter for the wettability, the roughness, is related directly to the growth parameters, which lead to excellent controllable and reproducible eutectic structures. Simply by varying etching time very high aspect ratios can be achieved, allowing studying the interaction of the very long needles with liquids. Moreover, the surface functionality can be tuned by RF-magnetron sputtering of PTFE onto the metal needles. As those layers can be very thin, our system allows, in principle, studying the transition from a metal to a polymer surface using submonolayers. Furthermore, the first contact angle measurements on the nanostructured and functionalized eutectic structures are presented and discussed.

Introduction

The water-repellent behavior of micro- and nanostructured plant surfaces,[1,2] the so-called Lotus effect, has inspired a significant amount of research on wettability of solid surfaces. A final objective is the realization of self-cleaning materials or switchable wettability.

Surface wettability is a property governed by both the chemical composition and the geometry of solid surfaces.[3,4] Depending on the contact angle, θ, surfaces can be classified as superhydrophilic ($\theta \approx 0°$), hydrophilic ($30° < \theta < 90°$), hydrophobic ($90° < \theta < 150°$), and superhydrophobic ($\theta > 150°$) (this nomenclature is valid if the liquid considered is water). Self-cleaning materials make use of the extreme situations, i.e., superhydrophilicity and superhydrophobicity. When a water droplet contacts a superhydrophilic surface it spreads out forming a thin film, whereas on a superhydrophobic surface it forms spherical drops to minimize the solid/liquid interface area. In the first case a thin layer of water runs off a surface, washing away dust by creeping underneath and thus cleaning the surface. In the case of a superhydrophobic surface, a water droplet rolls off the surface, carrying away contaminants and cleaning the surface.[5] Recently, theoretical calculations showed that significant tall structures are a precondition for an optimized liquid repellence[6] or even so-called "underwater superhydrophobicity".[7]

Superhydrophobic surfaces have usually been produced in two ways: on the basis of geometry and chemistry. In the geometric version, the method is to create a rough structure on a surface. The chemical route is to modify a rough surface with compounds with a low surface free energy, such as fluorinated or silicon compounds. It is possible to create roughness features out of hydrophobic materials as well.[8] Several superhydrophobic surfaces have been prepared using these approaches including fluoroalkylsilanes-modified inverse opal surfaces,[9] plasma polymerization,[10] anodic oxidation of aluminum,[11] gellike roughened polypropylene,[12] plasma fluorination of polybutadiene,[13] oxygen plasma-treated poly(tetrafluoroethylene),[14] densely packed aligned carbon nanotubes,[15] solidification of alkylketene dimer,[16] poly(dimethylsiloxane) (PDMS) by means of replica moulding,[17] and nanosphere lithography coupled with oxygen plasma etching.[18] In all experiments a common finding is that the water contact angle increases with surface roughness. However, in most of the techniques the nanostructures are limited by growth mechanisms and a high aspect ratio of the surface roughness cannot be achieved, which is required for advanced water repellence.[7,8] Therefore, to investigate how the nanometer features affect the wettability of a surface, the most difficult task is to fabricate and quantify nanostructures that can be systematically varied. In this study a novel route for preparing model samples for the quantitative investigation of the Lotus effect is shown. It consists of directional solidification and selective etching of

* To whom correspondence should be addressed. E-mail: hassel@elchem.de.

† Max-Planck-Institut für Eisenforschung GmbH.

‡ Christian-Albrechts-Universität.

(1) Neinhuis, C.; Barthlott, W. *Ann. Bot.* **1997**, *79*, 677.
(2) Barthlott, W.; Neinhuis, C. *Planta* **1997**, *202*, 1.
(3) Wenzel, R. N. *Ind. Eng. Chem.* **1936**, *28*, 988.
(4) Cassie, A. B. D.; Baxter, S. *Trans. Faraday Soc.* **1944**, *40*, 546.
(5) Blossey, R. *Nat. Mater.* **2003**, *2*, 301.
(6) Extrand, C. W. *Langmuir* **2006**, *22*, 1711.
(7) Marmur, A. *Langmuir* **2006**, *22*, 1400.
(8) Tavana, H.; Amirfazli, A.; Neumann, A. W. *Langmuir* **2006**, *22*, 5556.
(9) Gu, Z. Z.; Uetsuka, H.; Takahashi, K.; Nakajima, R.; Onishi, H.; Fujishima, A.; Sato, O. *Angew. Chem., Int. Ed.* **2003**, *42*, 894.
(10) Teare, D. O. H.; Spanos, C. G.; Ridley, P.; Kinmond ,E. J.; Roucoules, V.; Badyal, J. P. S. *Chem. Mater.* **2002**, *14*, 4566.
(11) Tsujii, K.; Yamamoto, T.; Onda, T.; Shibuchi, S. *Angew. Chem., Int. Ed.* **1997**, *36*, 1001.
(12) Erbil, H. Y.; Demirel, A. L.; Avci, Y.; Mert, O. *Science* **2003**, *299*, 1377.
(13) Woodward, I.; Schofield, W. C. E.; Roucoules, V.; Badyal, J. P. S. *Langmuir* **2003**, *19*, 3432.
(14) Morra, M.; Occhiello, E.; Garbassi, F. *Langmuir* **1989**, *5*, 872.
(15) Morra, M.; Occhiello, E.; Garbassi, F. *J. Colloid Inerface Sci.* **1989**, *132*, 504.
(16) Li, H.; Wang, X.; Song, Y.; Liu, Y.; Li, Q.; Jiang, L.; Zhu, D. *Angew. Chem. Int. Ed.* **2002**, *40*, 1743.
(17) Jopp, J.; Grüll, H.; Yerushalmi-Rozen, R. *Langmuir* **2004**, *20*, 10015.
(18) Shibuichi, S.; Onda, T.; Satoh, N.; Tsujii, K. *J. Phys. Chem.* **1996**, *100*, 19512.

10.1021/la0616303 CCC: $37.00
Published on Web 01/23/2007

Table 1. Geometry of Nanostructures

growth rate/ mm h^{-1}	growth rate/ μm s^{-1}	average diameter/ nm	average spacing/ μm	surface fraction/ % Re	total no. of wires	total area/ μm^2	wire density/ m^{-2}	roughness factor calculated for etching time of 900 s
200	55.5	328.6 ± 30	2.99 ± 0.3	1.81	86	728.4	11.8E+10	2.03
30	8.33	507.4 ± 35	4.61 ± 0.4	1.54	34	728.4	4.67E+10	1.40
5	1.39	713.9 ± 40	6.29 ± 0.5	1.29	21	728.4	2.88E+10	1.16

a NiAl−1.5 at. % Re eutectic alloy,[19] resulting in Re nanowire arrays with tunable geometry over a wide range. Moreover, functionalization of the resulting nanostructures is possible by poly(tetrafluoroethylene) (PTFE) sputtering. This allows a homogeneous coating of high aspect ratio surface structures as well as the possibility of fabricating ultrathin coatings, leading to a minimal thickening of the structures.

Experimental Section

Prealloys for directional solidification with composition NiAl−1.5 at. % Re were prepared from 99.97% Ni, 99.9999% Al, and a 99.9% Re by induction melting under an inert atmosphere. They were cast into a copper mould and placed in an alumina crucible. Directional solidification of the eutectic alloys was performed in a Bridgman-type crystal growth facility. The experiments were conducted with a constant temperature gradient of 40 K/cm and different growth rates (1−55 μm s^{-1}). Directionally solidified ingots were removed from the crucibles and cut in slices with a thickness of 1 mm by sparc erosion normal to the growth direction. They were prepared by grinding to grade 2400 SiC paper, mechanically polished down to grade 3 μm, and finally chemically polished with OPS suspension for further analysis.

Etching was performed in a mixture of HCl(32%):H_2O_2(30%):H_2O, 10:10:80, for various times as described in the next section. Scanning electron microscopy was performed on a LEO FE-SEM-type 1550 VP with a field emission gun.

Surface functionalization was carried out with a thin film coating of the metal with polymer. Poly(tetrafluoroethylene) (PTFE) was chosen due to its known high hydrophobic properties and high resistance to any chemical attack. As the deposition method, RF magnetron sputtering was chosen. The advantage of the sputter technique over other techniques in this case is the possibility to achieve excellent conformity over complex topography for a pinhole free coating and the possibility of a very controllable film thickness on relatively large substrates. A technological advantage is the high deposition rate, as demonstrated by RF magnetron deposition of different polymers.[20−22] Additionally, there are no problems with residual solvents such as in chemical deposition processes.

Deposition was performed in a metal vacuum chamber, which was initially evacuated to below 10^{-7} mbar. A Dressler CESAR 136 RF-Generator (13.560 MHz) is used to create the necessary RF field over the 2 in. polymer target on a cooled holder. An RF power of 50 W was applied to the PTFE target (deposition rate ≈ 10 nm/min). A nominal PTFE film thickness of 120 nm was deposited and carefully controlled by parallel deposition on silicon substrates and profilometer measurements. The polymer host shows a complete amorphous structure in the X-ray. It is known[23,24] that the sputtered polymer films have a completely different structure than pristine PTFE as observed with X-ray photoelectron spectroscopy (XPS). The C1s core-level spectra for pristine PTFE have only one peak at 292.0 eV due to the CF_2 groups in the polymer chains. After sputtering, the spectra show three additional peaks which are related to *C*F (290.2 eV, 28.1% fraction of C1s peak), *C*F_2 (292.0 eV, 31.7%), *C*F_3 (293.9 eV, 22.6%), and *C*−CF_x (287.9 eV, 17.6%) species.[25] The additional peaks are in agreement with pronounced cross-linking as reported earlier[21] for sputtered films. The cross-linking might be seen as an advantage in this case as it ensures higher mechanical stability of the polymer around the metal. The density of the sputtered PTFE was determined gravimetrically as 2.1 g/cm^3, which is close to the density given by the pristine polymer supplier (2.2 g/cm^3) taking into account the measurement error. Uniformity is checked by EDX (energy-dispersive X-ray spectrometry) in the scanning electron microscope by measuring the fluorine content of the film. The absence of pinholes is shown by deposition of ion-enriched water on top of the film. No current could be measured through the film after applying a voltage to the droplet and metal.

Contact angle measurements were conducted on a dataphysics contact angle system and recorded with a Teli CCD camera. Drops of deionized water (∼1 μL) were used to determine contact angles. Three different methods for contact angle determination are provided by the equipment: tangent searching, circle fitting, and ellipse fitting. All gave the same contact angles within the error.

Results and Discussion

NiAl−Re is a quasibinary alloy composed of a B2−NiAl phase and a hexagonal Re phase with a eutectic composition of 1.5 at. % Re. The invariant nature of eutectic reaction causes both phases to solidify simultaneously. This leads to a so-called coupled growth in which atoms rejected from one phase are consumed by the other phase and vice versa. In an attempt to minimize the surface energy, eutectics with a significantly asymmetric composition form nanofibers of a minor phase in a major phase.[26] This technique produces single crystals with embedded single-crystalline fibers all having the same crystallographic orientation.[27] Cross-sections of these 1-dimensionally structured samples are shown in Figure 1. Re fibers appear as bright spots in a darker NiAl matrix. It is seen that the fibers are very uniform in diameter and that the average spacing has a narrow distribution.[28] The growth rate was 5 mm h^{-1} in Figure 1a, 30 mm h^{-1} in Figure 1b, 200 mm h^{-1} in Figure 1c. The average nanowire diameter and spacing changed accordingly from 714 to 507 to 329 nm for the diameter and 6.29 to 4.61 to 2.99 μm for the spacing. It should be emphasized that wire diameter and spacing cannot be changed independently. They are directly correlated to each other by the volume ratio in the eutectic. Formation of a regular structure of these fibers is directly linked to the eutectic composition and processing conditions. The figures shown are 2-dimensional projections of the volume fraction of the eutectic alloy.

To determine the wire density *n*, that is the number of wires *N* per area *A*, the wires observed in Figure 1a−c were counted. There were 21, 34, and 86 wires counted on the investigated area of 728 μm^2. This means that wire densities *n* of 2.88×10^{10}, 4.67×10^{10}, and 11.8×10^{10} m^{-2} are found. All values are summarized in Table 1.

(19) Hassel, A. W.; Bello Rodriguez, B.; Milenkovic, S.; Schneider, A. *Electrochim. Acta* **2005**, *51*, 795.
(20) Fukushima, K.; Ikeda, Y.; Hayashi, T.; Kikuchi, N.; Kusano, E.; Kinbara, A. *Thin Solid Films* **2001**, *392*, 254.
(21) Biederman, H. *J. Vac. Sci. Technol. A* **2000**, *18*, 1642.
(22) Biederman, H.; Zeuner, M.; Zalman, J.; Bilkova, P.; Slavinska, D.; Stelmasuk, V.; Boldyreva, A. *Thin Solid Films* **2001**, *392*, 208.
(23) Yang, G. H.; Zhang, Y.; Kang, E. T.; Neoh, K. G. *J. Phys. Chem. B* **2003**, *107*, 2780.
(24) Golub, M. A.; Wydeven, T.; Johnson, A. L. *Langmuir* **1998**, *14*, 2217.
(25) Schürmann, U.; Hartung, W. A.; Takele, H.; Zaporojtchenko, V.; Faupel, F. *Nanotechnology* **2005**, *16*, 1078.
(26) Jackson, K. A.; Hunt, J. D. *Trans. Met. Soc. AIME* **1966**, *236*, 1129.
(27) Kurz, W.; Sahm, E. *Gerichtet erstarrte eutektische Werkstoffe* **1975** (Springer, Berlin).
(28) Milenkovic, S.; Hassel, A. W.; Schneider, A. *Nano Lett.* **2006**, *6*, 794.

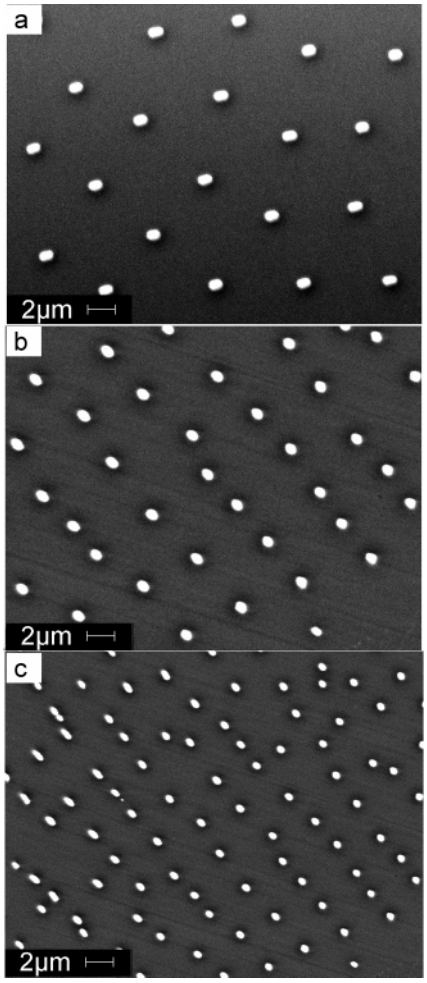

Figure 1. Micrographs (SEM) of directionally solidified NiAl−Re eutectics processed at different growth rates of (a) 5 (1.39 μm s^{-1}), (b) 30 (8.33 μm s^{-1}), and (c) 200 mm h^{-1} (55.5 μm s^{-1}). Geometrical parameters such as the average wire diameter, average spacing, and wire density are summarized in Table 1.

Three-dimensional structuring of this material is possible by a selective dissolution of one of the phases. Electrodissolution of the minor phase is possible in a neutral buffer in which the NiAl forms a stable passive aluminum oxide layer, whereas Re dissolves into the solution as perrhenate.[29] For studies on the Lotus effect an alternate process is more interesting in which the major phase is dissolved to release a nanofiber array. This is accomplished in an etching solution consisting of 80 mL of H_2O, 10 mL of HCl, and 10 mL of H_2O_2. The etching rate in this solution is approximately 6 nm s^{-1} or 0.36 μm min^{-1}. An example for an etching time of 5 min is shown in Figure 2. Rhenium fibers are partly released from the matrix. All fibers are parallel to each other, having the same length and a uniform diameter all over the length. These features together with the fact that they are single-crystalline metal and provide both a narrow distribution in average diameter and average spacing make this system interesting as a model system for studying the Lotus effect. In contrast to some other model systems investigated so far,[30] this system enables submicrometer dimensions and extreme aspect ratios and it is self-organized, which significantly reduces the number of fabrication steps.

The wetting characteristics of surfaces are influenced by surface roughness, which is usually described through the roughness factor, r, defined as the ratio of actual surface area over the projected area. For the nanofiber array shown in Figure 2, assuming that each nanofiber has a cylindrical shape, the roughness factor can be expressed as

$$r = 1 + \pi dl/\lambda^2 \quad (1)$$

where d is the diameter, l is the length of the wires, and λ is the spacing between them. The length of the wires is the product of the etching rate e_r and the etching time t

$$l = e_r t \quad (2)$$

For a given temperature gradient the diameter of the wires depends on the growth rate

$$d = K_1 v^{-0.5} \quad (3)$$

where K_1 is a material constant and v is the growth rate.[28] As stated before, the spacing, λ, also depends on the growth rate

$$\lambda = K_2 v^{-0.5} \quad (4)$$

For the NiAl−Re system the constants K_1 and K_2 were determined to be 1.63 × 10^{-9} and 1.48 × 10^{-8} m$^{1.5}$ s$^{0.5}$, respectively.[28] Hence, substituting eqs 2−4 in eq 1 the relationship between the surface roughness and processing parameters is obtained

$$r = 1 + K_3 v^{0.5} e_r t \quad (5)$$

where K_3 has a value of 0.257. In this way the geometry of the samples and roughness can be directly derived from processing parameters such as growth rate and etching time. Thus, it allows simple control of the parameters to study the influence of the geometry on hydrophobicity.

To prove the suitability of the Teflon-coated metal needles as a model system for quantitative examination of the Lotus effect, first contact angle measurements are performed. Figure 3 shows

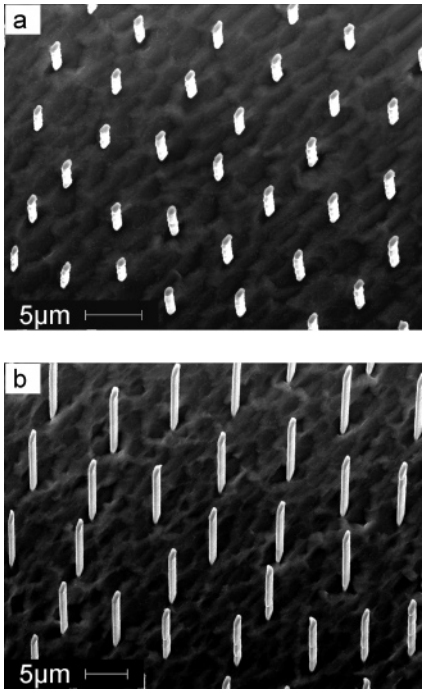

Figure 2. Micrograph (SEM) of directionally solidified NiAl−Re eutectics etched for (a) 5 and (b) 15 min in a HCl/H_2O_2 mixture; details are given in the text.

(29) Bello Rodriguez, B.; Hassel, A. W.; Schneider, A. *J. Electrochem. Soc.* **2006**, *153*, C33.
(30) Öner, D.; McCarthy, T. J. *Langmuir* **2000**, *16*, 7777.

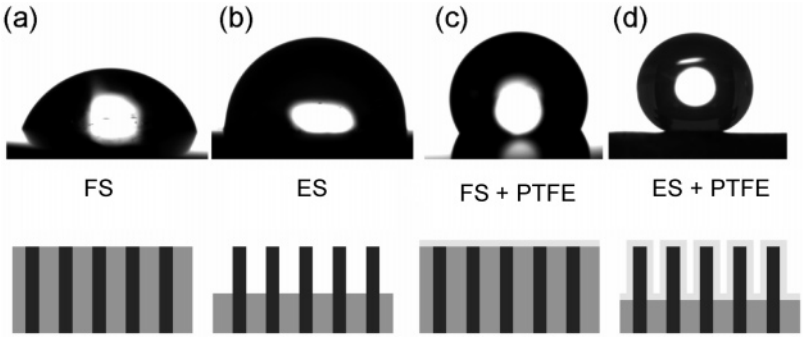

Figure 3. Photographs during contact angle measurement: (a) flat NiAl−Re eutectic surface (FS); (b) etched surface with 2 μm long Re wires (ES); (c) flat eutectic surface coated with 120 nm PTFE (FS + PTFE); (d) etched and PTFE-coated surface (ES + PTFE); superhydrophobicity can be observed.

four contact angle measurements of different droplets on the systematically modified surfaces. The contact angle observed in Figure 3a originates from the flat eutectic surface (FS). It is in the hydrophilic region and is 70.9°. The effect of the etched structure (ES) can be seen in Figure 3b. The contact angle is significantly increased. The Re wires were 20 μm long, and a pronounced change in the contact angle at the bottom is visible. This points to the beginning of a Wenzel-like hydrophobic behavior. The contact angle of the flat surface coated with PTFE (FS + PTFE) is 120°, within experimental error, as shown in Figure 3c. For comparison, the substrate is the same as in part a of the figure. The PTFE coating of the etched structure (ES + PTFE) with the Re wires shown in part b exhibits superhydrophobicity. The contact angle is larger than 165°; a more precise measurement is difficult due to the typical increase of angle toward the interface. Usually contact angle determination is performed by tangent searching, circle fitting, and ellipse fitting. The maximum error of this procedure is determined to be less than 5°. Note that this cannot be performed if very long needles are used. This can be seen from Figure 4. Here, even a change in the slope of the droplet near the surface can be observed. At the position of the arrowhead, the slope changes from convex to concave. This requires consideration of two contact angles as indicated in the sketch, which are $\theta_1 = 86°$ and $\theta_2 = 65°$.

In an attempt to visualize the effects surface structure and surface functionality have on the contact angle, the results of these measurements were plotted in Figure 4b. The contact angle θ ranges from superhydrophilic 0° to superhydrophobic 180°. This figure demonstrates that the range of contact angles that can be achieved by functionalization of a metallic surface spans a wider range as compared to silicon or polymer structures.[31] The etchant used in production of the nanowire arrays contains oxidizing agents. Thus, a few nanometer thick oxide film will form on the metal, decreasing the hydrophilicity. It can be expected that a subsequent chemical reduction of the surface would lower the contact angle even further.

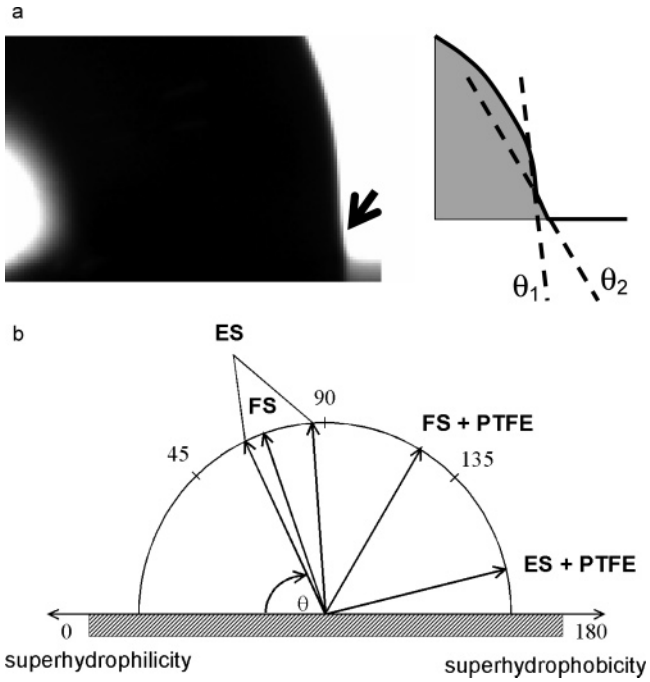

Figure 4. (a) Magnification of the side of a droplet on the rhenium nanowires. A change in the droplet shape can be observed right at the interface to the needles (see arrow). This change has an influence on the contact angle determination, as depicted in the sketch. (b) Influence of the surface structure and functionalization on the contact angle.

Conclusion

In summary, a very controllable model system for study of the wettability of surfaces is introduced. By using a directionally solidified and selectively etched eutectic, needlelike surfaces of predetermined roughness were fabricated. The surface roughness could be directly related to the growth parameters of the eutectic alloy. The length of the needles can be individually adjusted by the choice of the etching time. Needles as long as 100 μm were produced.[32] The length is usually only limited by a bending of the wires at these extreme aspects ratios of 500 or more. In the experiments presented here only 2 μm long needles were shown. The surface functionality was tuned by RF-magnetron sputtering of PTFE onto the metal needles. First contact angle measurements showed the extreme influence of both the surface structure and the surface functionalization including superhydrophobicity. Therefore, it is concluded that the model system introduced here is very suitable for investigating the influence of structure and surface functionalization on the wettability.

Acknowledgment. Financial support of the Deutsche-Forschungs-Gemeinschaft through the projects Production of Nanowire Arrays through Directional Solidification and their Application and Strain Aligned Nanowires on Insulating Substrates within the DFG Priority Programme 1165 Nanowires and Nanotubes−From Controlled Synthesis to Function is gratefully acknowledged.

LA0616303

(31) Yoshimitsu, Z.; Nakajima, A.; Watanabe, T.; Hashimoto, K. *Langmuir* **2002**, *18*, 5818

(32) Hassel, A. W.; Smith, A. J.; Milenkovic, S. *Electrochim. Acta* **2006**, *52*, 1799.